ACS APPLIED MATERIALS & INTERFACES

Letter

www.acsami.org

Inkjet Printing Controllable Footprint Lines by Regulating the Dynamic Wettability of Coalescing Ink Droplets

Meijin Liu,[†] Jingxia Wang,[†] Min He,*[,†] Libin Wang,[†,‡] Fengyu Li,[†] Lei Jiang,[†] and Yanlin Song*[,†]

[†]Beijing National Laboratory for Molecular Sciences (BNLMS), Center for Molecular Sciences, Key Laboratory of Green Printing, Key Laboratory of Organic Solids, Institute of Chemistry, Chinese Academy of Sciences, Beijing 100190, P. R. China

[‡]University of Chinese Academy of Sciences, Beijing 100049, P. R. China

Supporting Information

ABSTRACT: Inkjet printing lines with controllable footprints is the prerequisite of fabricating high-quality patterns. However, achieving precise footprints of lines by inkjet printing is still a challenge because of the difficulty in controlling coalescences of ink droplets. Here, controllable footprint lines were fabricated by adjusting the ink droplets' dynamic wettability which is depended on the ink droplets' surface tension difference. The experimental surface tension difference of 0.77−1.50 mN/m leads to appropriate surface dynamic wettability to ink droplets and the formation of straight lines, which agrees well with the theoretical results. These results will pave the way for printing electronics and patterns.

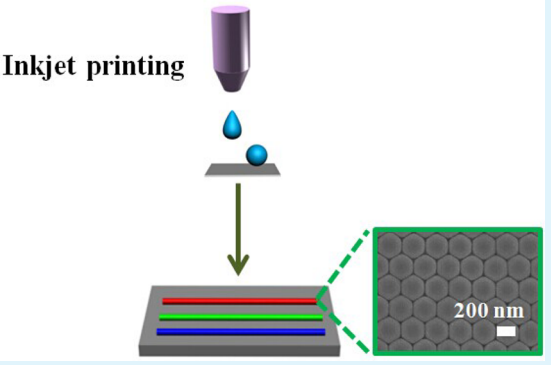

KEYWORDS: *controllable footprint line, inkjet printing, coalescence, dynamic wettability*

Fabricating high-quality patterns is an attractive issue for promising applications in fields of photoelectric devices.[1−4] In recent years, inkjet printing technology has become a facile and promising approach to fabricate well-designed patterns because of its easy combination of directing writing, high throughput, low cost, and self-assembly of micro/nano structures,[5−8] whereas the dot-on-demand printing mode leads to uncontrollable footprints of patterns that are quite adverse to high-performance photoelectric devices. Efforts have been done to solve this problem in the past decades. Some investigations showed that the droplet space played a preliminary role in the formation of lines,[8−10] attention has also been focused on the high wettability substrates with fine pore structures,[11] the laser-induced forward transfer,[12] and the drops' viscosities.[13] However, controlling footprints of inkjet printing lines is still a challenge, especially for those consisted of functional nanoparticles, e.g. photonic crystal (PC) lines. Recently, Lee et al.[14] suggested that controlling ink droplets' coalescence could be used to tailor the structures of inkjet-printed materials, Karpitschka and Riegler[15] reported that the different drop surface tension affected the coalescence of two drops. In addition, Subramaniam et al.[16] and Chen et al.[17] showed that the interfacial jamming of nanoparticles had great influence on the drops' coalescence behavior. However, little attention has been paid to the surface dynamic wettability during the coalescence of ink droplets, which is crucial to the evolution of their footprints.

Herein, controllable footprint lines were fabricated by inkjet printing based on the coalescence of ink droplets because of their different dynamic wettability on substrates. By changing ink droplets' surface tension and the nanoparticle concentration simultaneously, ink droplets showed different dynamic wettability on substrates, which dominated the coalescence of ink droplets and the final footprints of lines. As a result, spherical caps, lines and dumbbells were obtained. The disclosed intrinsic influence of the surface dynamic wettability on coalescences of ink droplets counts much in constructing controllable footprints of lines. These results throw new lights on fabricating sensors and photoelectric devices with high quality and controllable patterns by synergistic combining the self-assembly and inkjet printing.

Figure 1 presents three typical cases of coalescing ink droplets (Figure 1A_1, B_1, C_1) due to the distinguishing dynamic wettability of droplet 1 on substrates. In the present experiments, the solvent of the ink is the mixture of water and ethylene glycol (EG), which were used to adjust the ink droplet's surface tension and the nanoparticle concentration because of the different evaporating rate and surface tension of water and EG. Here, the nanoparticle concentration refers to the volume ratio of nanoparticles occupying the air−liquid−solid three-phase contact region. Different surface tension and nanoparticle concentration dominate distinguishing dynamic wettability of ink droplets on the substrate. For the first case, the surface tension of droplet 1 is similar to that of the droplet

Received: July 1, 2014
Accepted: August 9, 2014
Published: August 9, 2014

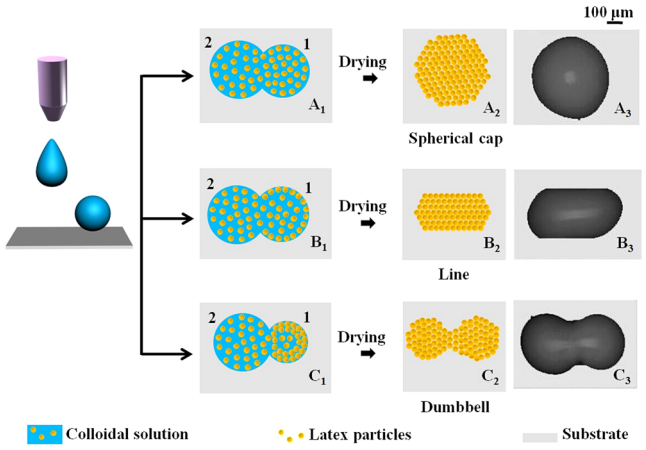

Figure 1. Three typical coalescing cases of the neighboring ink droplets induced by different dynamic wettabilities of ink droplets on the substrates. Because of (A_1, B_1, C_1) the difference in surface tension and nanoparticle concentration, the dynamic wettabilities of ink droplets on the substrates were different, resulting in (A_2, A_3) spherical cap, (B_2, B_3) continuous line, and (C_2, C_3) dumbbell structure after coalescing and drying. (A_3, B_3, C_3) Optical images of coalesced ink droplets forming spherical cap, line, and dumbbell structure, respectively.

2 and no particles assembly occurs at the three-phase contact line (TCL), which leads to the easy depinning TCL of the droplet 1 and similar dynamic wettability to the droplet 2. After coalescing and drying, a spherical cap is obtained (Figure 1A_2). The optical image demonstrates the formed footprint of the coalesced ink droplet (Figure 1A_3). For the second and third cases, the surface tension of droplet 1 is smaller than that of the droplet 2 because of the fast evaporation of water. Moreover, nanoparticles assemble at the TCL of the droplet 1, which pins the TCL and favors the formation of straight line after coalescing and drying (Figure 1B_1, B_2). More nanoparticles assembling at the TCL lead to stronger pinning TCL and the dumbbell formation (Figure 1C_1, C_2). These processes are demonstrated by the optical images in Figure 1B_3, C_3.

The evolution of the surface tension and the assembly of nanoparticles at the TCL were investigated to disclose the different dynamic wettability of ink droplet on a substrate during its drying (Figure 2). After an ink droplet impacting on a substrate by inkjet printing, its footprint spreads, retracts and finally pins on the substrate (Figure 2A).[18] The detailed dynamic behavior of an ink droplet was recorded by a high-speed camera (see Figure S1 in the Supporting Information). Accompanied by the solvent's evaporation,[19] the nanoparticles assembled along the TCL and the liquid–gas interface driven by the capillary force and convective effects.[20,21] Finally, the droplet dried and kept a sphere-cap structure (Figure 2A). According to the equation $\gamma_{drop} = (62.79-0.26t)/(1-3.61 \times 10^3 t)$ (please see the Supporting Information for details), with the increasing evaporating time, the ratio of water to EG in the solvent decreased and the surface tension of ink droplets decreases (Figure 2B). The well-ordered nanoparticle assembly at the surface of the ink droplet was confirmed by the strengthening reflection and blue-shift of peak position during the evaporation (Figure 2B and Figure S2 in the Supporting Information). The increasing reflection is attributed to the assembling nanoparticles at the drop surface, whereas the blue-shift of peak position from 662 to 576 nm is resulted from more close-packed structures of the nanoparticles (see Figure S2 in the Supporting Information).[22] Assuming that the structure of nanoparticles at the drop surface were homogeneously dispersed in the suspension before drying, and the structure is isotropically shrunk with the solvent evaporation without any loss in generality, the nanoparticle volume ratio (f) can be calculated with the equation $f = (4.55D)/(1.52\lambda\cos((\pi-\theta)/3))$ based on the Bragg's law[23] (D is the diameter of particles in ink; λ is the maximum reflection wavelength; θ is the incidence angle, and θ =90° in our experiments; see the Supporting Information for details). The results imply that the nanoparticle concentration increases when the evaporating time prolongs (Figure 2C and Figure S3 in the Supporting Information). The theoretical results further solidify the nanoparticle assembly at the TCL during the solvent evaporation. More importantly, the assembling nanoparticles will pin the TCL of liquid droplets.[21] Consequently, with different evaporating time 0, 15, 30, and 45 s, the advancing angles of ink droplets are 84.2 ± 2.7, 87.0 ± 2.9, 96.3 ± 3.1, and 120.6 ± 5.8°, and the receding angles are 40.3 ± 2.2, 34.2 ± 3.7,

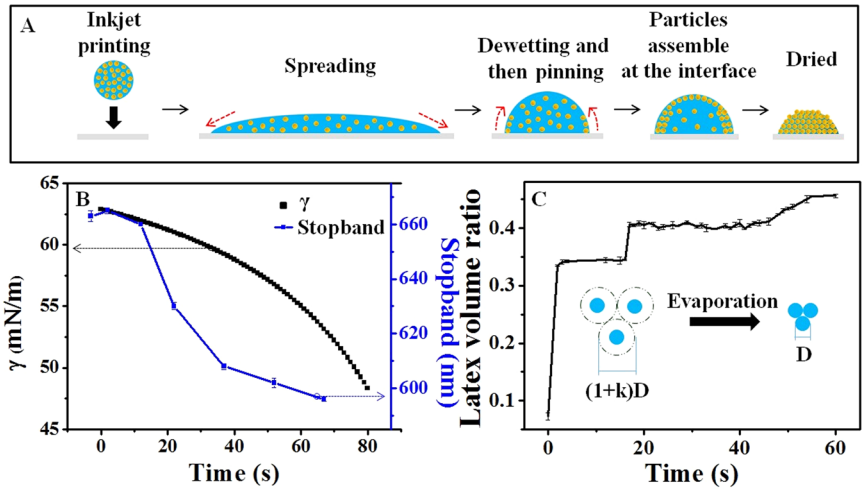

Figure 2. (A) Schematic wetting and dewetting behavior of a single ink droplet after impacting on a substrate. (B) Evolutions of the surface tension and stopband position of single ink droplet with increasing evaporation time. (C) Relationship of the nanoparticle concentration of inkjet droplet with evaporation time, the surface tension decreases, whereas the nanoparticle concentration increases with the prolonging evaporation time.

dx.doi.org/10.1021/am5042548 | ACS Appl. Mater. Interfaces 2014, 6, 13344–13348

16.3 ± 1.2, and 4.9 ± 1.6°, respectively. The contact angle (CA) was measured with a CA measurement device (OCA20, DataPhysics, Germany) by dropping a 1 μL ink droplet onto the substrate. The advancing CA of an ink droplet on the substrate was measured as soon as the footprint slipped forward when more ink was added into the droplet.[24] Similarly, the receding CA was measured as soon as the footprint slipped backward when some ink was removed from the droplet. Each reported CA was an average of five independent measurements. The varying advancing and receding angles indicate the different dynamic wettability of ink droplets on the substrate, which dominates the coalescence behavior of ink droplets as well as their footprints according to the in situ observations.

To clarify the formation of different footprints during the coalescence of ink droplets, we carried out the in situ observations of three typical coalescences (Figure 3A–C).

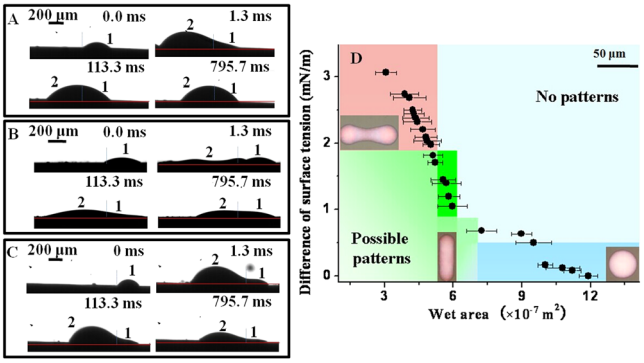

Figure 3. (A–C) Optical images of the coalescing ink droplets forming spherical caps, lines, and dumbbells, respectively. (D) Different footprints formed by coalescing ink droplets with different dynamic wettability on the substrate. Blue, green, and magenta sections signify spherical caps, lines and dumbbells respectively, the solid cycles are experimental results. Increasing surface tension difference leads to distinguished dynamic wettability of two coalescing ink droplets, which is advantageous for forming dumbbells.

After the first ink droplet (droplet 1) sat on the substrate, the second ink droplet (droplet 2) fell, impacted and spread on the substrate subsequently. The extended TCL of droplet 2 met droplet 1 and coalesced. It should be noted that the surface tension and the nanoparticle concentration were altered by controlling the evaporating time during inkjet printing. For the case of forming a spherical cap, the evaporating time of the first ink droplet was ∼15 s when the coalescence occurs. The coalesced droplets vibrated for several microseconds and a spherical droplet finally formed (Figure 3A and Movie 1 in the Supporting Information). For the cases of forming a line and a dumbbell structure, the evaporating time of the first ink droplet were about 30 and 40 s, respectively, when the coalescence occurs. The TCL on one side of the coalesced droplet pinned on the surface for all the cases except that forming a spherical cap (Figure 3B, C and Movies 2 and 3 in the Supporting Information), whereas the TCL on the opposite side depinned and moved forward. The different behavior of the TCL during coalescences can be ascribed to the different dynamic wettability of the substrate to ink droplets, which was induced by the varying surface tension and nanoparticle concentration.

The energy transformation among the surface energy, kinetic energy, adhesion and gravity during coalescences deform the coalescing droplet and drive the TCL movement. In order to speculate the energy dissipation induced by dynamic viscidity of ink droplets, the *Re* number (defined as $Re = \rho vR/\eta$) and the *We* number (defined as $We = \rho v^2 R/\gamma$) were calculated, which are ∼789.05 and ∼51.1, respectively (ρ is 0.9857 g/mL, the velocity (v) is 1 m/s, η is 4.06 mPa s, R is 325 μm, and γ is 62.79 mN/m). It should be noted that in the present work, the Reynolds number (Re = 145.0) is much larger than unit even when the water evaporates completely (when water evaporates completely, the solvent is EG and the viscosity of the ink drop is 22.1 mPa s). Both of the *Re* number and the *We* number are much larger than unit, indicating the energy dissipation can be ignored during the coalescences.[25] Considering the energy change during the coalescence of two ink droplets, the surface energy of the first ink droplet at the time of coalescence can be obtained as $\gamma_A S_A = \gamma_{co}(1 + \cos\theta_{adv})S_{co,wetting} + \gamma_{co}(1 + \cos\theta_{rec})S_{co,dewetting} + \gamma_{co}S_{co,s} - C$ based on different dynamic wettability of the two ink droplets to the substrate indicated by the advancing and receding angles. Here, γ_A and S_A refer to the surface tension and the surface area of the first ink droplet, respectively. γ_{co} is the surface tension of the coalescing droplet and equal to the surface tension of the second ink droplet without any loss in generality because the capillary flow and Marangoni flow[26] reconstruct the droplet surface. θ_{adv}, θ_{rec} are the advancing and receding angles of the second ink droplet, respectively. $S_{co,\ wetting}$, $S_{co,\ dewetting}$ are the wetting and dewetting area of the coalesced droplet on the substrate, $S_{co,\ S}$ is the surface area of the coalesced droplet, C is determined by the inkjet printing experiments and includes the gravity potential energy, kinetic energy, and surface energy of the second ink droplet (please see the Supporting Information for details). According to the equation, the receding contact angle dominates the footprint behavior of coalesced droplets. The evolution of coalesced droplets' footprints is shown in Figure 3D. With the increasing surface tension difference, the receding contact angle of the droplet 1 decreases and consequently, two ink droplets will coalesce to form spherical caps, lines and dumbbells (marked by blue, green, and magenta color, respectively, in Figure 3D). When the surface tension difference of two ink droplets is smaller than 0.49 mN/m, spherical caps will form after they coalescing, whereas lines will be obtained as the surface tension difference is in the range 0.89–1.89 mN/m. If the surface tension difference is larger than 1.89 mN/m, just dumbbells form after two neighboring ink droplets coalesced. These agree well with the experimental results that the corresponding surface tension differences to form spherical caps, lines and dumbbells are <0.77, 0.77–1.50, and >1.50 mN/m, respectively (showed with solid cycles in Figure 3D). The theoretical and experimental results solidify the effect of the dynamic wettability on the coalescences of ink droplets and the coalesced footprints thereof.

Considering the effect of dynamic wettability on the footprints, lines with different footprints, such as straight line and wave line, were inkjet printed with inks containing poly(styrene-methyl methacrylate-acylic acid) (poly(St-MMA-AA), simplified as PS) (Figure 4A, C, E), silicon dioxide (see Figure S4 in the Supporting Information) or silver nanoparticles (Figure 4B, D). Figure 4A is the optical image of a line consisted of PS nanoparticles with wave footprint. The inset in Figure 4A is the scanning electron microscope (SEM) image of the printed line consisted of PS (the average diameter of PS nanoparticles is 272 nm). The SEM image showed perfect orderly self-assembly of PS nanoparticles after drying by inkjet printing, which is vital to fabricate high quality devices by inkjet

dx.doi.org/10.1021/am5042548 | ACS Appl. Mater. Interfaces 2014, 6, 13344–13348

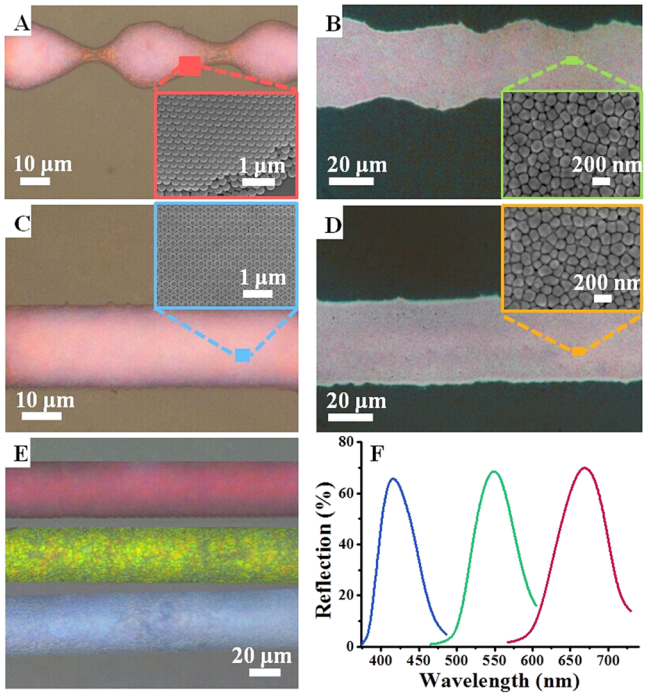

Figure 4. Optical microscope images of the as-printed PC lines with (A) wave and (C) straight footprints, silver lines with (B) wave and (D) straight footprints. Three typical straight PC lines (red, green, and blue) demonstrating (E) good optical properties and (F) micro-reflectance spectra of the printed PC lines; the insets are the corresponding SEM images. PC lines in A, C, and E show vivid structure color due to the well-ordered nanoparticle assembly.

printing. Other nanoparticles, such as silicon dioxide nanoparticles (see Figure S4 in the Supporting Information, the average diameter is 330 nm) and silver nanoparticles (the average diameter is 111 nm) were also chosen to fabricate lines with straight footprints (see Figure S4 in the Supporting Information and Figure 4D) and wave footprint (Figure 4B). As it is well-known that inkjet printing straight lines play important roles in constructing desired patterns and high quality devices. Here, in addition to inkjet printing controllable footprint lines with ink containing different nanoparticles, continuous PC lines consisted of different size nanoparticles were also inkjet printed by controlling the dynamic wettability of coalescing ink droplets (Figure 4E). The optic microscope images show vivid structure color (Figure 4E) because of the well-ordered nanoparticle assembly (inset in Figure 4C). Three typical continuous homogeneous PC lines with straight footprints, the red, green and blue lines demonstrating high optic properties (Figure 4F), with the stopband positions of 680, 570, and 480 nm were obtained by corresponding nanoparticle diameters of 272, 210, and 193 nm.

In summary, by adjusting ink droplets' surface tension and the nanoparticle concentration, different dynamic wettability of ink droplets to substrates were achieved and subsequently spherical caps, lines, dumbbells were obtained by inkjet printing. The intrinsic influence of the dynamic wettability of ink droplets to substrates on the coalescing dynamic behavior was clarified. The ranged experimental surface tension difference of 0.77−1.50 mN/m leads to the appropriate dynamic wettability of ink droplets to the substrate for the formation of straight lines consisted of nanoparticles, which agrees well with the theoretical results. The intrinsic relation between the dynamic wettability and the final patterns is important to guide the coalescence of ink droplets containing nanoparticles. Moreover, the inkjet printed PC lines show good optical properties due to the well-ordered assembly of nanoparticles. These results will be of significance to inkjet print nanoparticles for high-quality patterns and devices.

■ ASSOCIATED CONTENT

Supporting Information

This material is available free of charge via the Internet at http://pubs.acs.org.

■ AUTHOR INFORMATION

Corresponding Authors

*E-mail: ylsong@iccas.ac.cn.
*E-mail: heminyiwen@iccas.ac.cn.

Notes

The authors declare no competing financial interest.

■ ACKNOWLEDGMENTS

We gratefully acknowledge financial support from the NSFC (Grants 51173190, 21003132, 21073203, 91127038, 21121001, and 21303220), the 973 Program (2013CB933004, 2011CB932303, and 2011CB808400), the "Strategic Priority Research Program" of the Chinese Academy of Sciences (Grant XDA09020000).

■ REFERENCES

(1) Lei, Y.; Yang, S. K.; Wu, M. H.; Wilde, G. Surface Patterning Using Templates: Concept, Properties and Device Applications. *Chem. Soc. Rev.* **2011**, *40*, 1247−1258.

(2) Hwang, J. K.; Cho, S.; Dang, J. M.; Kwak, E. B.; Song, K.; Moon, J.; Sung, M. M. Direct Nanoprinting by Liquid-Bridge-Mediated Nanotransfer Moulding. *Nat. Nanotechnol.* **2010**, *5*, 742−748.

(3) Ok, J. G.; Park, H. J.; Kwak, M. K.; Pina-Hernandez, C. A.; Ahn, S. H.; Guo, L. J. Continuous Patterning of Nanogratings by Nanochannel-Guided Lithography on Liquid Resists. *Adv. Mater.* **2011**, *23*, 4444−4448.

(4) Ok, J. G.; Kwak, M. K.; Huard, C. M.; Youn, H. S.; Guo, L. J. Photo-Roll Lithography (PRL) for Continuous and Scalable Patterning with Application in Flexible Electronics. *Adv. Mater.* **2013**, *25*, 6554−6561.

(5) Kuang, M. X.; Wang, L. B.; Song, Y. L. Controllable Printing Droplets for High-Resolution Patterns with Uniform Morphology. *Adv. Mater.* **2014**, DOI: 10.1002/adma.201305416.

(6) Kim, H.; Ge, J. P.; Kim, J.; Choi, S. E.; Lee, H.; Lee, H.; Park, W.; Yin, Y. D.; Kwon, S. Structural Colour Printing Using a Magnetically Tunable and Lithographically Fixable Photonic Crystal. *Nat. Photonics* **2009**, *3*, 534−540.

(7) Kuang, M. X.; Wang, J. X.; Wang, L. B.; Song, Y. L. Research Progress of High-quality Patterns by Directly Inkjet-Printing. *Acta Chim. Sin.* **2012**, *70*, 1889−1896.

(8) Park, J.; Moon, J. Control of Colloidal Particle Deposit Patterns within Picoliter Droplets Ejected by Ink-Jet Printing. *Langmuir* **2006**, *22*, 3506−3513.

(9) Oh, Y.; Yoon, H. G.; Lee, S. N.; Kim, H. K.; Kim, J. Inkjet-Printing of TiO_2 Co-Solvent Ink: from Uniform Ink-Droplet to TiO_2 Photoelectrode for Dye-Sensitized Solar Cells. *J. Electrochem. Soc.* **2012**, *159*, B35−B39.

(10) Soltman, D.; Subramanian, V. Inkjet-Printed Line Morphologies and Temperature Control of the Coffee Ring Effect. *Langmuir* **2008**, *24*, 2224−2231.

(11) Kim, C.; Nogi, M.; Suganuma, K.; Yamato, Y. Inkjet-Printed Lines with Well-Defined Morphologies and Low Electrical Resistance on Repellent Pore-Structured Polyimide Films. *ACS Appl. Mater. Interfaces* **2012**, *4*, 2168−2173.

(12) Palla-Papavlu, A.; Córdoba, C.; Patrascioiu, A.; Fernández-Pradas, J. M.; Morenza, J. L.; Serra, P. Deposition and Characterization of Lines Printed Through Laser-Induced Forward Transfer. *Appl. Phys. A: Mater. Sci. Process.* **2013**, *110*, 751−755.
(13) Lee, M. W.; Kima, N. Y.; Chandra, S.; Yoona, S. S. Coalescence of Sessile Droplets of Varying Viscosities for Line Printing. *Int. J. Multiphase Flow* **2013**, *56*, 138−148.
(14) Ihnen, A. C.; Petrock, A. M.; Chou, T.; Fuchs, B. E.; Lee, W. Y. Organic Nanocomposite Structure Tailored by Controlling Droplet Coalescence during Inkjet Printing. *ACS Appl. Mater. Interfaces* **2012**, *4*, 4691−4699.
(15) Karpitschka, S.; Riegler, H. Noncoalescence of Sessile Drops from Different but Miscible Liquids: Hydrodynamic Analysis of the Twin Drop Contour as a Self-Stabilizing Traveling Wave. *Phys. Rev. Lett.* **2012**, *109* (066103), 1−5.
(16) Subramaniam, A. B.; Abkarian, M.; Mahadevan, L.; Stone, H. A. Non-Spherical Bubbles. *Nature* **2005**, *438*, 930−930.
(17) Chen, G.; Tan, P.; Chen, S. Y.; Huang, J. P.; Wen, W. J.; Xu, L. Coalescence of Pickering Emulsion Droplets Induced by an Electric Field. *Phys. Rev. Lett.* **2013**, *110* (064502), 1−5.
(18) Kim, H.; Lee, C.; Kim, M. H.; Kim, J. Drop Impact Characteristics and Structure Effects of Hydrophobic Surfaces with Micro- and/or Nanoscaled Structures. *Langmuir* **2012**, *28*, 11250−11257.
(19) Arcamone, J.; Dujardin, E.; Rius, G.; Francesc, P. M.; Ondarcuhu, T. Evaporation of Femtoliter Sessile Droplets Monitored with Nanomechanical Mass Sensors. *J. Phys. Chem. B* **2007**, *11*, 13020−13027.
(20) Deegan, R. D.; Bakajin, O.; Dupont, T. F.; Huber, G.; Nagel, S. R.; Witten, T. A. Capillary Flow as the Cause of Ring Stains from Dried Liquid Drops. *Nature* **1997**, *389*, 827−829.
(21) Weon, B. M.; Je, J. H. Self-Pinning by Colloids Confined at a Contact Line. *Phys. Rev. Lett.* **2013**, *110* (028303), 1−5.
(22) Ge, J. P.; Goebl, J.; He, L.; Lu, Z. D.; Yin, Y. D. Rewritable Photonic Paper with Hygroscopic Salt Solution as Ink. *Adv. Mater.* **2009**, *21*, 4259−4264.
(23) Richel, A.; Johnson, N. P.; McComb, D. W. Observation of Bragg Reflection in Photonic Crystals Synthesized from Air Spheres in a Titania Matrix. *Appl. Phys. Lett.* **2000**, *76*, 1816−1818.
(24) Erbil, H. Y.; McHale, G.; Rowan, S. M.; Newton, M. I. Determination of the Receding Contact Angle of Sessile Drops on Polymer Surfaces by Evaporation. *Langmuir* **1999**, *15*, 7378−7385.
(25) Hyvaluoma, J.; Timonen, J. Impact States and Energy Dissipation in Bouncing and Non-Bouncing Droplets. *J. Stat. Mech.: Theory Exp.* **2009**, *2009* (P06010), 1−10.
(26) Scriven, L. E.; Sternling, C. V. Marangoni Effects. *Nature* **1960**, *187*, 186−188.